Drug Development and Industrial Pharmacy, 31:191–207, 2005

ISSN: 0363-9045 print / 1520-5762 online
DOI: 10.1081/DDC-200047806

Taylor & Francis
Taylor & Francis Group

Novel Modulation of Drug Delivery Using Binary Zinc-Alginate-Pectinate Polyspheres for Zero-Order Kinetics Over Several Days: Experimental Design Strategy to Elucidate the Crosslinking Mechanism

Viness Pillay and Michael P. Danckwerts
Department of Pharmacy and Pharmacology, University of the Witwatersrand, Johannesburg, Gauteng, South Africa

Zayniddin Muhidinov and Reza Fassihi
Department of Pharmaceutical Sciences, Temple University, School of Pharmacy, Philadelphia, Pennsylvania, USA

ABSTRACT A Box-Behnken design was applied to mathematically establish whether different degrees of crosslinking were induced by Zn^{2+} and Ca^{2+} ions in polyspheres composed of alginate and/or pectin, and the model drug ibuprofen. Based on their different crystal structures and coordination numbers, a theoretical model was proposed demonstrating that Zn^{2+} ions preferentially crosslink alginate and pectin. In addition, the lower coordination number of Zn^{2+} (4–6) would significantly retard hydration of both polymers, as opposed to Ca^{2+} (7–9). The responses studied for 28 statistically derived polyspheres included drug encapsulation efficiency, physicomechanical behavior, and in vitro drug release potential. Single-tailed Student's t-tests on data generated for the encapsulation efficiencies, primary facture values, and rupture energies indicated that Zn^{2+} was statistically superior ($p < 0.05$) in crosslinking alginate and pectin. Further textural analysis revealed a good correlation between the Brinell hardness number and fracture load, while an inverse relationship was found for matrix tensile strength. Viscosity studies demonstrated different in situ crosslinking thresholds for Zn^{2+}. The Durbin-Watson statistic and correlation coefficient revealed that the quadratic regression function was highly accurate in predicting the responses. Using a generalized reduced gradient algorithm on dissolution values obtained after 2 hours (t_{2h}) provided optimized solutions for achieving zero-order release extending from 2 hours to 7 days. Mathematical simulations projected drug release from 25 to 50 days.

KEYWORDS Box-Behnken design, Alginate-pectin, Crosslinking, Zinc-calcium, Drug encapsulation, Physicomechanical behavior, In vitro release, Numerical optimization

Address correspondence to Professor Viness Pillay, Department of Pharmacy and Pharmacology, University of the Witwatersrand, 7 York Road, Parktown 2193, Johannesburg, Gauteng, South Africa. Fax: +27-11-642-4355; E-mail: pillayvi@therapy.wits.ac.za

INTRODUCTION

Crosslinked polymers, in contrast to their native structures, are differentiated by their dimensional stability and enhanced thermal, physicochemical, and physicomechanical characteristics, particularly in their ability to orientate their three-dimensional configuration. The hydrational dynamics of crosslinked matrices are highly complex and consequently have a significant impact on their gelation rates (Kjoniksen et al., 2003; Pillay & Fassihi, 2001; Pillay et al., 2002.). In this regard, gelation can be viewed in the context of critical phenomena and percolation, and hence motivated many researchers to compare the scaling exponents with a large variety of phase transitions (Crichton & Surita, 2003; Terentjev et al., 2003; Tiitu et al., 2002). Related developments have also taken place in the case of reversible gelation where the junction zones of the polymeric network are formed due to noncovalent interactions such as helical domains, microcrystalline bundles, hydrogen bonding, coordination, hydrophobic effects, and other physical interactions.

Researchers in areas such as metallurgy, engineering, and food chemistry have extensively studied the interaction of alginates and pectins with various metal ions (Braccini et al., 1999; Debon & Tester, 2001; Franco et al., 2002; Ibanez & Umetsu, 2002; Jang et al., 1999). Specifically, Zn^{2+} and Ca^{2+} ions have been reported to bind at different sites at alginate (McDowell, 1979). In this regard, it has only been speculated that Zn^{2+} ions are less selective and hence produce more extensive crosslinking (Aslani & Kennedy, 1996a).

In the area of drug delivery, the application and selectivity of Zn^{2+} and Za^{2+} ions for alginate has to date been inconclusive. Gray and Dowsett (1988) have shown that the release of insulin was more retarded from crosslinked Zn-alginate beads in comparison to Ca-alginate. However, Aslani and Kennedy (1996a) have alluded to this mechanism being an interaction between Zn^{2+} and insulin, not alginate. Furthermore, these researchers have also concluded that the use of Zn^{2+} as a crosslinking ion in alginate appears to offer no advantages compared to Ca^{2+}, at least in the context of controlling the diffusion of acetaminophen from gel films. In an ensuing study, it was reported that Zn-alginate beads released paracetamol more slowly than Ca-alginate beads in water (100% dissolution in 4–5 h), while complete dissolution was observed in simulated gastric fluid within 2 h, and unaffected by the cation type (Aslani & Kennedy, 1996b). Except for Zn-alginate beads, paracetamol was released rapidly in citrate solution. Biopharmaceutically, this may be considered inappropriate based on the sequential pH changes within the gastrointestinal fluid and the role of gastric emptying time (Wilding et al., 2001). Furthermore, all release profiles followed first-order kinetics. The same conclusion was reached for the interaction of Zn^{2+} and Ca^{2+} ions with pectin (Dronnet et al., 1996). Chan et al. (2002), using an emulsification method, reported that alginate microspheres could not be successfully produced with ZnSO4 as the sole crosslinking agent—a combination of $CaCl_2$ and $ZnSO_4$ was essential. Even the inclusion of Zn^{2+} ions, drug release was not significantly lower in comparison to microspheres prepared only with Ca^{2+} ions, and simply followed squareroot kinetics. El-Gibaly (2002) showed that the release of ketoprofen from Zn-pectinate microparticles and tablets provided slow with almost complete release ($\approx$80%) over 8–30 h, and a lag-phase ranging from 5–20 h. This system was highly suitable as an alternative carrier for colonic drug delivery.

The objective of this study was to apply a statistical experimental design as an accurate tool to elucidate the different degrees of crosslinking associated with Ca^{2+} and Zn^{2+} ions. Specifically, spherical, ionotropically crosslinked binary Zn-alginate-pectinate multiparticulate matrices (referred to as "polyspheres" in this study) were developed to establish a platform for rate-controlled, zero-order delivery of ibuprofen utilizing a Box-Behnken design. The application of this optimization technique would provide an efficient and economical method to acquire the necessary information to understand the relationship between the controllable (independent) and performance (dependent) variables that affect crosslinking (Bonferoni et al., 2000; Furlanetto et al., 2003; Prakobvaitayakit & Nimmannit, 2004). The study proposed a theoretical understanding for the superior crosslinking effect of Zn^{2+} over the traditional Ca^{2+} ion based on their spatial geometry and orientation, as well as on data derived from physicomechanical and physicochemical investigations. In order to demonstrate the mechanistic influence of crosslinking, zinc sulfate heptahydrate ($ZnSO_4.7H_2O$) and zinc gluconate ($C_{12}H_{22}ZnO_{14}$) were selected to react with a binary alginate-pectin

polymeric system. The varying responses that were investigated as a result of crosslinking included the textural properties, drug encapsulation efficiency, in vitro release potential, changes in viscosity, and compressional characteristics of the polyspheres.

MATERIALS AND METHODS

A low-viscosity sodium alginate (35 cP for a 1% w/v aqueous solution at 21°C) was obtained from TIC Gums (Belcamp, MD, USA). Low methoxyl citrus pectin (DE ≈ 34–38%) was donated by Herbstreith and Fox (Neuenburg/Wurttemberg, Germany). Anhydrous calcium chloride ($CaCl_2$), zinc sulfate heptahydrate ($ZnSO_4.7H_2O$), and Zn gluconate ($C_{12}H_{22}ZnO_{14}$) USP were purchased from Spectrum (New Brunswick, NJ, USA). Ibuprofen USP was purchased from Sigma (St. Louis, MO, USA).

Formulation of Crosslinked Zinc-Alginate-Pectine Polyspheres

Drug-loaded polyspheres were formulated in accordance with the Box-Behnken design, having polymer and crosslinking agent concentrations in statistical combinations as depicted in Tables 1 and 2. Note that the design is based on three levels i.e., a lower, middle, and upper value.

The formulation of the crosslinked polyspheres was conducted in a similar manner described elsewhere (Pillay & Danckwerts, 2002). Briefly, the polyspheres were produced by titration of a polymer-drug suspension at 1 mL/min into the crosslinking solution by means of a peristaltic pump through a flat-tipped, 14-gauge needle based on the combinations presented in Table 2. The polyspheres were agitated in the crosslinking solution for an additional 15 min, followed by curing at room temperature (±21°C) for 24 h. After curing, the crosslinking solution was decanted, polyspheres were washed with 2 × 400 mL deionized water and dried under an extractor (±18°C) for 48 h.

The quadratic response model with 15 terms Eq. 1 generated from the above design included 24 experimental runs and four center points:

$$\begin{aligned}\text{Response} = {} & b_0 + b_1 * \text{NaAl} + b_2 * \text{P} + b_3 \\ & * \text{ZnS} + b_4 * \text{ZnG} + b_5 * \text{NaAl} \\ & * \text{NaAl} + b_6 * \text{P} * \text{P} + b_7 * \text{ZnS} \\ & * \text{ZnS} + b_8 * \text{ZnG} * \text{ZnG} + b_9 \\ & * \text{NaAl} * \text{P} + b_{10} * \text{NaAl} * \text{ZnS} \\ & + b_{11} * \text{NaAl} * \text{ZnG} + b_{12} * \text{P} * \text{ZnS} \\ & + b_{13} * \text{P} * \text{ZnG} + b_{14} * \text{ZnS} * \text{ZnG} \quad (1)\end{aligned}$$

where the concentrations of sodium alginate and pectin are represented by NaAl and P, and the concentrations of the crosslinkers $ZnSO_4.7H_2O$ and $C_{12}H_{22}ZnO_{14}$ are represented by ZnS and ZnG. $b_0 \ldots\ldots b_{14}$ are the regression coefficients.

Determination of Polysphere Drug Encapsulation

The concentration of total drug entrapped within the polyspheres was determined by dissolving 100-mg samples in triplicate in phosphate buffer pH 6.8. Upon dissolution of the polyspheres, 5-mL samples of each solution were filtered using a Millipore® filter (0.45 μm pore size). The total drug content was thereafter measured by UV at a wavelength of 230 nm. Note that it was established at the outset that the polymers and excipients did not interfere with drug analysis at 230 nm. The absorbance was converted to a concentration value using a standard curve (y =

TABLE 1 Lower and Upper Factor Levels of the Independent Variables for the Box-Behnken Design

	Factor levels		
Variable	Lower level	Upper level	Units
Sodium alginate (NaAl)	0	2	%w/v
Pectin (P)	0	2	%w/v
Zinc sulfate heptahydrate (ZnS)	0	5	%w/v
Zinc gluconate (ZnG)	0	5	%w/v

TABLE 2 Box-Behnken Matrix for the Production of Different Combinations of Crosslinked Zinc-Alginate-Pectinate Polyspheres

Polysphere number P#	Randomized run order	[NaAl] (%w/v)	[P] (%w/v)	[ZnS] (%w/v)	[ZnG] (%w/v)
1	17	0	1	2.5	0
2	12	1	0	2.5	5
3	5	1	1	5	5
4[a]	9	1	1	0	0
5[b]	24	0	0	2.5	2.5
6	2	2	0	2.5	2.5
7	1	1	2	2.5	0
8	11	1	1	2.5	2.5
9	13	0	2	2.5	2.5
10	20	0	1	5	2.5
11	10	1	0	2.5	0
12	3	1	2	5	2.5
13	6	1	0	0	2.5
14	4	1	1	2.5	2.5
15	25	2	1	5	2.5
16	7	1	1	0	5
17	15	1	1	2.5	2.5
18	19	2	2	2.5	2.5
19	23	1	2	0	2.5
20	21	1	0	5	2.5
21	27	1	1	2.5	2.5
22	8	1	2	2.5	5
23	14	0	1	0	2.5
24	16	2	1	0	2.5
25	28	2	1	2.5	0
26	22	0	1	2.5	5
27	26	2	1	2.5	5
28	18	1	1	5	0

[a]P4 could not be crosslinked since there were no crosslinking ions.
[b]P5 could not be crosslinked since there were no polymers.

43.004×-0.0029, $R^2 > 0.99$), and the percentage drug encapsulation was calculated from Eq. 2:

$$\text{Drug Encapsulation}\,(\%) = (\text{AQ}/\text{TQ}) \times 100 \qquad (2)$$

where AQ is the actual quantity of drug entrapped within the polyspheres and TQ is the theoretical quantity of drug that should have been entrapped within the polyspheres.

In order to validate the method of drug analysis, several parameters were calculated. Inter- and intra-day precision (RSD%) for ibuprofen were well within $\pm 1.5\%$, and accuracy within 98.4–101.2%. Repeatability and reproducibility were found to be excellent, within an RSD of $<1\%$. The limit of detection and limit of quantitation in phosphate buffer pH 6.8 were 0.02 and 0.08 mg/mL.

TABLE 3 Textural Settings Employed for Resilience, Work Performed During Rupture, and Degree of Primary Fracture Associated with Matrix Rupture

	Settings	
Test parameters	Matrix resilience	Matrix rupture energy and primary fracture value
Test speed	0.2 mm/s	0.2 mm/s
Compressive force/distance	50% strain	60 N
Sensitivity of trigger force	0.005 N	0.005 N

Textural Profiling of Crosslinked Zinc-Alginate-Pectinate Polyspheres

Textural analysis was employed to characterize the resilient nature of the polyspheres (i.e., resistance to deformation), the work performed during complete rupture of the matrix (i.e., complete disruption/breakage of a brittle material), and the degree of primary fracture just prior to matrix rupture (i.e., the first point at which the matrix begins to crack) using the *TA.XTplus* Texture Analyzer (Stable Micro Systems, England) fitted with a 10-mm cylindrical steel probe and a 5-kg load cell. Note that all polyspheres uniformly dried to a hard yet brittle consistency, which allowed for the measurement of total breakage without separating the process into plastic and elastic deformation. In addition, none of the formulations remained spongy in nature.

The settings used to calculate the above parameters are depicted in Table 3 below.

Typical force-displacement/time profiles generated for the calculation of the textural parameters are shown in Fig. 1.

Figure 1a depicts the points used in the calculation of matrix resilience, which is provided by the ratio of the AUC between anchors 2 and 3, and 1 and 2. Figure 1b indicates the calculation of the energy required for matrix rupture, which is provided by the totao AUC for a force-distance profile (i.e., AUC between anchors 1 and 2).

Figure 1c depicts the phase of first deflection (primary fracture) in the upward gradient, which indicates the primary fracture phase just prior to matrix rupture. This value is calculated from the steepness of the positive gradient up to the point of first force deflection, namely between anchors 1 and 2.

The resilient nature of hydrated polyspheres was also determined. In this case, 100 mg of polyspheres were hydrated in 250 mL phosphate buffer pH 6.8 maintained at 37°C. At 0.5, 1, 2, 3, 4, and 5 hours, 10 polyspheres were removed and subjected to resilience measurements using the parameters outlined in Table 3.

In addition, two other parameters related to matrix integrity were calculated. The fracture load was determined on a Pharmatron AG tester with modified platens to accommodate individual unhydrated polyspheres. Both the stationary and movable platens were extended by the addition of perfectly right-angled

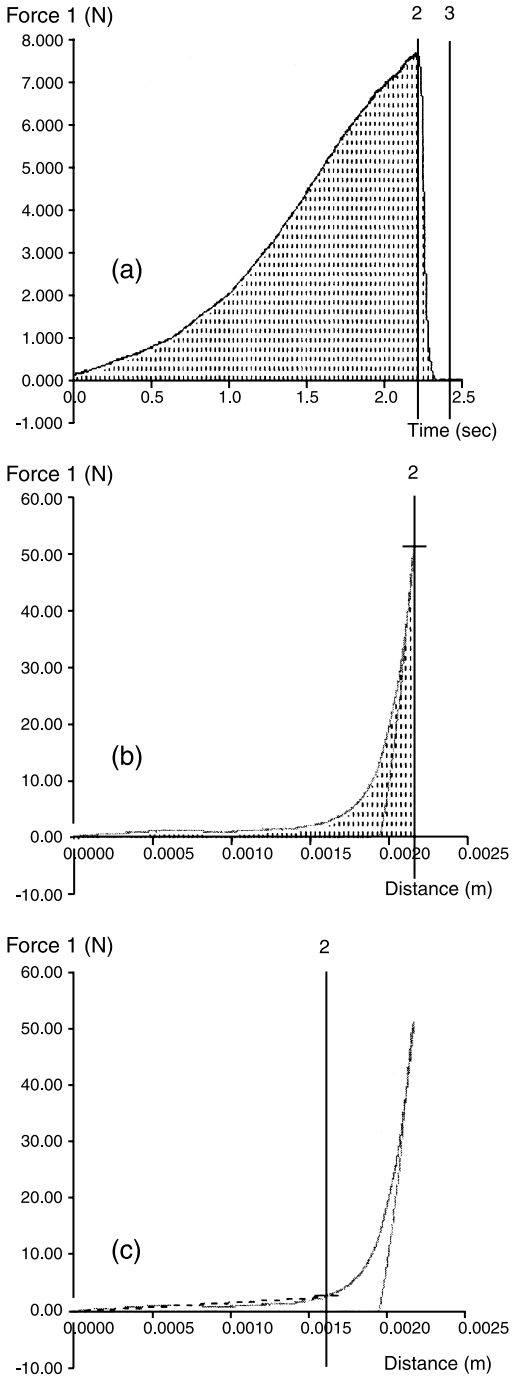

FIGURE 1 **Typical Textural Force-Time and Force-Distance Profiles of Crosslinked Zinc-Alginate-Pectinate Polyspheres for the Determination of (a) Matrix Resilience, (b) Matrix Rupture Energy, and (c) Primary Fracture Value. (N=10, S.D. <0.1 in All Cases).**

stainless steel metal strips having a thickness of 3 mm. The instrument was calibrated to ensure validation of the method. An accuracy of ±0.13% was established. In addition, each measurement was performed 10 times on single different polyspheres of the same formulation (N=10) to ensure accuracy of the readings. Using the

TABLE 4 Polymer, Drug, and Crosslinker Combinations Used for Viscosity Measurements

Experimental run	[NaAl] (%w/v)	[P] (%w/v)	[Ibuprofen] (%w/v)	[ZnS] (%w/v)	[ZnG] (%w/v)
1	1	0	0.5	2.5	0
2	1	0	0.5	0	2.5
3	1	0	0.5	2.5	0
4	0	1	0.5	2.5	0
5	0	1	0.5	0	2.5
6	0	1	0.5	2.5	2.5
7	1	1	0.5	2.5	0
8	1	1	0.5	0	2.5
9	1	1	0.5	2.5	2.5
10	1	0	0	2.5	0
11	1	0	0	0	2.5
12	1	0	0	2.5	2.5
13	0	1	0	2.5	0
14	0	1	0	0	2.5
15	0	1	0	2.5	2.5
16	1	1	0	2.5	0
17	1	1	0	0	2.5
18	1	1	0	2.5	2.5

ball probe indentation method, the Brinell hardness number (BHN) of unhydrated polyspheres was calculated using Eq. 3:

$$\mathrm{BHN} = 2F/\pi D(D^2 - d^2)^{1/2} \qquad (3)$$

where F=force generated from indentation, D=diameter of ball probe indenter (0.5 mm), and d=indentation depth (0.25 mm).

Determination of the Changes in the Viscosity of the Polymers During In Situ Crosslinking

Viscosity transitions of sequentially crosslinking solutions of sodium alginate and/or pectin were evaluated with or without ibuprofen. These transitions were measured using a novel method that traced the increasing changes during polymeric entanglement (Brookfield Viscometer, RV Spindle #2). While the homogenized polymer and/or drug suspensions were gently stirred, incremental μL quantities of crosslinker(s) were added. The 18 combinations of polymers and crosslinkers analyzed are listed in Table 4.

Polymer and/or drug suspensions were gently allowed to stir for 5 min. Thereafter, the beaker was removed from its magnetic stirrer, allowed to equilibrate for 1 min, after which the viscosity was read at 50 rpm. During the testing process, 2 min were allowed for the viscometer reading to stabilize (CV $<$ 0.05% acceptance criteria). The polymer(s) and/or drug suspension was replaced on the stirrer and 500 μL of the crosslinker solution(s) was added, allowed to stir for a further 5 min, followed by a 1-min equilibration period after which the viscosity was retested.

In Vitro Release Studies

In vitro dissolution studies (Caleva Dissolution Apparatus, model 7ST) were performed in triplicate on a quality of polyspheres equivalent to 200 mg of ibuprofen using the USP 25 rotating paddle method at 50 rpm in 900 mL phosphate buffer pH 6.8 maintained 37°C. Samples of 5 mL were withdrawn by an autosampler (Hewlett Packard) over predetermined time intervals and analyzed by UV at 230 nm.

RESULTS AND DISCUSSION

Proposed Theoretical Mechanism of the Superior Crosslinking Effects of Zn^{2+} over Ca^{2+} Ions in Alginate and Pectin Polymeric Systems

In general, crosslinking has been associated with the salting-out potential of different ions, as arranged in

the Hofmeister series. As an analogy, this can be described in a manner in which ions preferentially bind to hydrating groups on the surface of enzymes in comparison to binding with polymer monomers. Therefore, the concentration of hydrating groups is reduced and thus the solubility of the protein (or polymer as in this study) is significantly hindered.

Chaplin (2004) published an extensive article on the Hofmeister series associated with the structure of water and its behavior. Some excerpts from this insightful work are employed in the following discussion. Ions such as SO_4^{2-} and $ZnBr_4^{2-}$ form a hydrated zone consisting of small rings of hydrogen bonded water molecules (Mayanovic et al., 2001; Plumridge et al., 2000). Such a zone may consist of a symmetrical dodecahedral arrangement of 16 molecules of water where each SO_4^{2-} oxygen is hydrogen bonded to three water molecules. Such molecules form small looped chains of two [six occurrences per SO_4^{2-} $(H_2O)_{16}$] or three [12 occurrences per $SO_4^{2-}(H_2O)_{16}$] molecules from one oxygen of SO_4^{2-} to another (Wang et al., 2001).

However, one of the complexities associated with the above-mentioned ability of clusters to interact with a water dodecahedron is related to significantly different aqueous properties of SO_4^{2-} and, as another example, ClO_4^- ions. Typically, these two ions are located at extreme ends of the Hofmeister series. However, the ClO_4^- ions appear in an expanded clathratelike water dodecahedra while SO_4^{2-} appears in a collapsed, puckered water dodecahedra. This difference is due to the lack of the oxygen atoms in ClO_4^- to form strong hydrogen bonds, thereby allowing it to fit within a complete dodecahedral water clathrate shell (Havel & Hogfeldt, 1995; Lavelle & Fresco, 2003).

Using the above theory as a platform for the present study, a review of the structural geometry of Ca^{2+} and Zn^{2+} provides a very interesting perspective on their interaction within the three-dimensional pockets formed by sequences in which the monomeric units of alginate and pectin are arranged. Ca^{2+} has a rigid, hexagonally close-packed shape (Fig. 2a). In its divalent form it has an ionic radius of 114 pm (atomic volume of 29.9 cm^3/mol). On the other hand, Zn^{2+} has a distorted, hexagonally close-packed shape (Fig. 2b). In its divalent form it has an ionic radius of 88 pm (atomic volume of 9.2 cm^3/mol) (Ionic Information of Calcium, 2004; Ionic Information of Zinc, 2004).

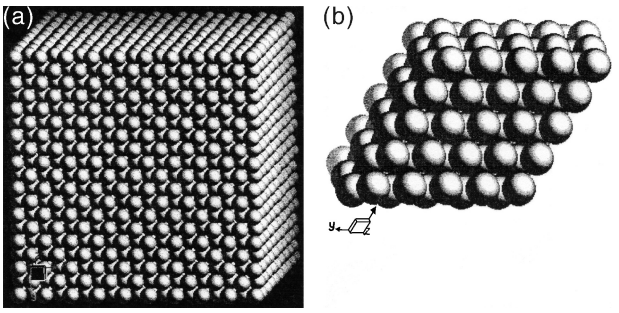

FIGURE 2 **Crystal Structures of (a) Ca^{2+} and (b) Zn^{2+} Ions. Actual Magnification of the Zn^{2+} Ion is Scaled Down by a Value of 1.39 Based on the Ionic Radius Ratio of Ca^{2+} 144 pm: Zn^{2+} 88 pm Ratio (Crystal Structure of Calcium, 2004; Crystal Structure of Zinc, 2004).**

Polymeric chain rigidity, as in the case of alginate and pectin, and their binary mixture thereof, would depend on the intimate proximity of the counter crosslinking ions with each other and the monomeric units. Closer proximity would enhance their interaction with the pendant molecules, hence increasing chain stiffness.

Based on the hexagonally rigid structure of Ca^{2+} in conjunction with its larger atomic volume (and ionic radius), it appears that this data would not suitably fit into the three-dimensional pockets of the polymeric chains as indicated in Fig. 3. However, in the case of Zn^{2+}, the distortion of its hexagonal structure, in conjunction with its smaller atomic volume (and ionic radius), would enhance the manner in which the ion fits into the polymeric pockets (Fig. 3). In addition, we believe that the distorted structure of Zn^{2+} enables more ions to fit within these pockets, achieving thermodynamic stability and hence, having a greater effect in reducing chain mobility. Another important consequence of having more Zn^{2+} ions within the polymeric pockets suggests that fewer water molecules are able to infiltrate and thus the degree of hydration is significantly lower, compared to when Ca^{2+} is used.

In conjunction with the above hypothesis, important energetics data on the binding of water molecules to Ca^{2+} and Zn^{2+} ions were found based on the examination of their coordination preferences in accordance with the Cambridge Structural Database (CSD) and ab initio molecular orbital calculations (Bock et al., 2003; George et al., 2003). Ca^{2+} ions bind with a higher coordination number, having values of 7-9 in crystal structures. Oxygen is the preferred ligand, hence water is easily attracted. On the other hand, Zn^{2+} ions

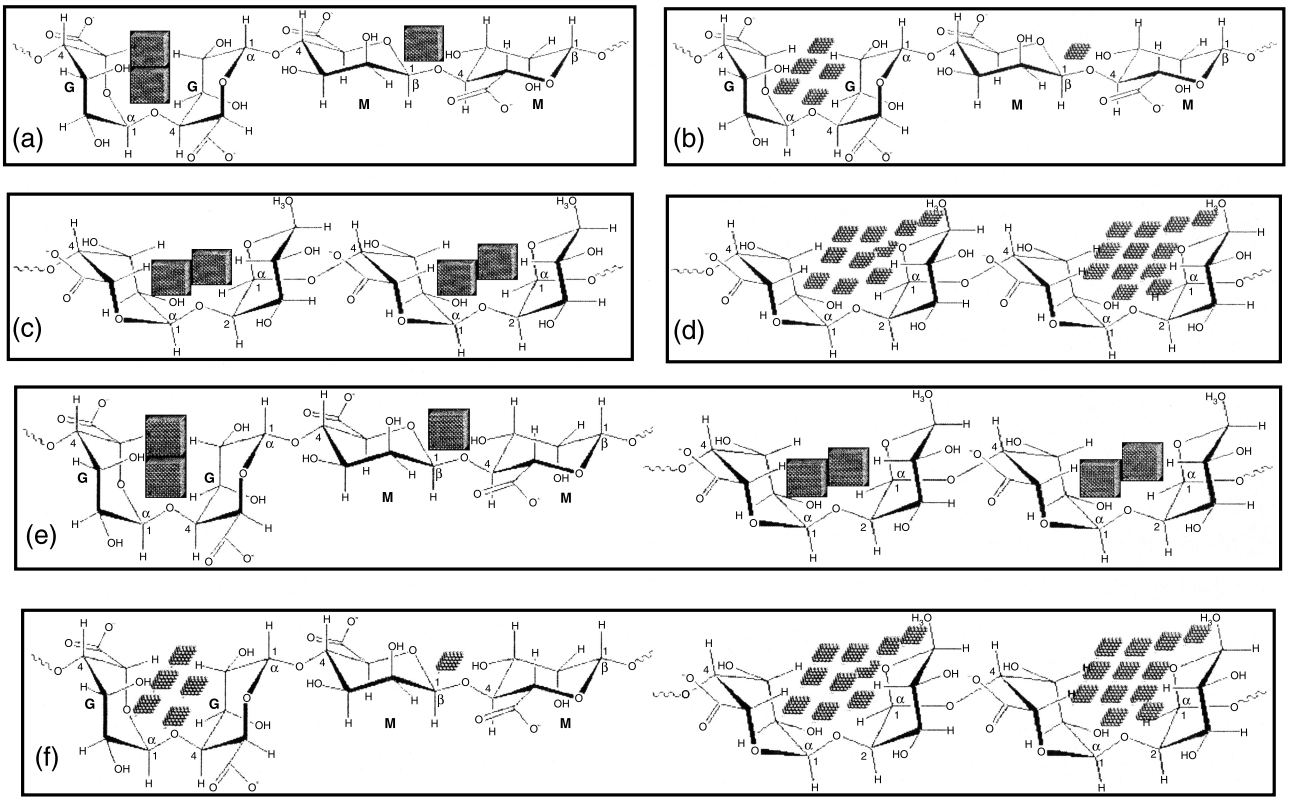

FIGURE 3 **Proposed Schematic Representation of the Structural Orientation in the Binding of (a) Ca^{2+} Ions to Mannuronic (MM) and Guluronic (GG) Acid Residues of Alginate, (b) Zn^{2+} Ions to MM and GG Acid Residues of Alginate, (c) Ca^{2+} Ions to Galacturonic Acid (GU) Residues of Pectin, (d) Zn^{2+} Ions to GU Residues of Pectin, (e) Ca^{2+} Ions to the GG, MM, and GU Residues of a Binary Mixture of Alginate and Pectin, and (f) Zn^{2+} Ions to the GG, MM, and GU Residues of a Binary Mixture of Alginate and Pectin.**

with the same charge are more flexible, and also bind to oxygen. However, the smaller coordination number, varying between 4–6, lowers its water-attracting power. Therefore in this regard, we believe that in order to obtain a greater degree of polymeric crosslinking with the added benefit of reduced hydration, it appears that Zn^{2+} is preferred over Ca^{2+}. From a pharmaceutical perspective, greater crosslinking and lower hydration of the polymer may substantially reduce the rate of drug release from such a matrix. Based on this information, it is hypothesized that the crosslinking of pectin by Zn^{2+} ions (Fig. 3d) will be superior to any other combination presented in Fig. 3–highest chain immobilization and lowest hydration. This hypothesis provides an alternative explanation to that proposed by El-Gibaly (2002). Proof of concept will be illustrated later.

Drug Encapsulation Efficiency

Figure 4 indicates the drug encapsulation efficiency for all crosslinked polyspheres.

A statistical comparison of the drug encapsulation efficiency of the alginate and pectinate crosslinked polymers as well as the $ZnSO_4.7H_2O$ and $C_{12}H_{22}ZnO_{14}$ as crosslinking ions was made. The

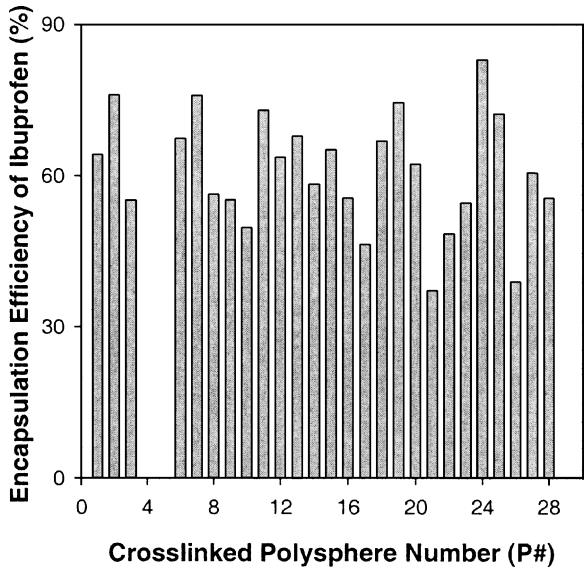

FIGURE 4 **Ibuprofen Encapsulation for Efficiency Within Crosslinked Matrices (N = 10, S.D. < 0.12 in All Cases).**

results indicate that the combination of pectin and Zn^{2+} ions was less efficient in entrapping drug (average of 52.58% entrapped) as compared to the alginate and Zn^{2+} ion combination (average of 69.36% entrapped). A single-tailed, Student's t-test calculated this difference to be significant ($p=0.0078$). This lower encapsulation efficiency of the pectinate polyspheres was attributed to the more effective crosslinking by the Zn^{2+} ions. Therefore, it is apparent tha the three-dimensional polymeric structure is occupied by a greater concentration of Zn^{2+} ions, leaving minimal network space for the entrapment of drug. In addition, the lower atomic weight of Zn^{2+} (65.39 g/mol) gains preference in occupying the polymeric matrix as oposed to the relatively large structure of ibuprofen ($C_{13}H_{18}O_2$), which has a molecular weight of 206.28 g/mol. The atomic and molecular weight of the ions and drug respectively, additionally support the above-mentioned relating to the atomic volume and coordination numbers.

As far as the crosslinking ability of the two different forms of Zn^{2+} ions is concerned (from $ZnSO_4.7H_2O$ and $C_{12}H_{22}ZnO_{14}$), no significant difference was found in their reaction with pectin ($p=0.9911$) or sodium alginate ($p=0.8956$).

Textural Profiling Analysis of the Crosslinked Polyspheres

The polyspheres produced were spherical in nature. Size determination by sieve analysis exhibited a unimodal distribution curve with the majority of

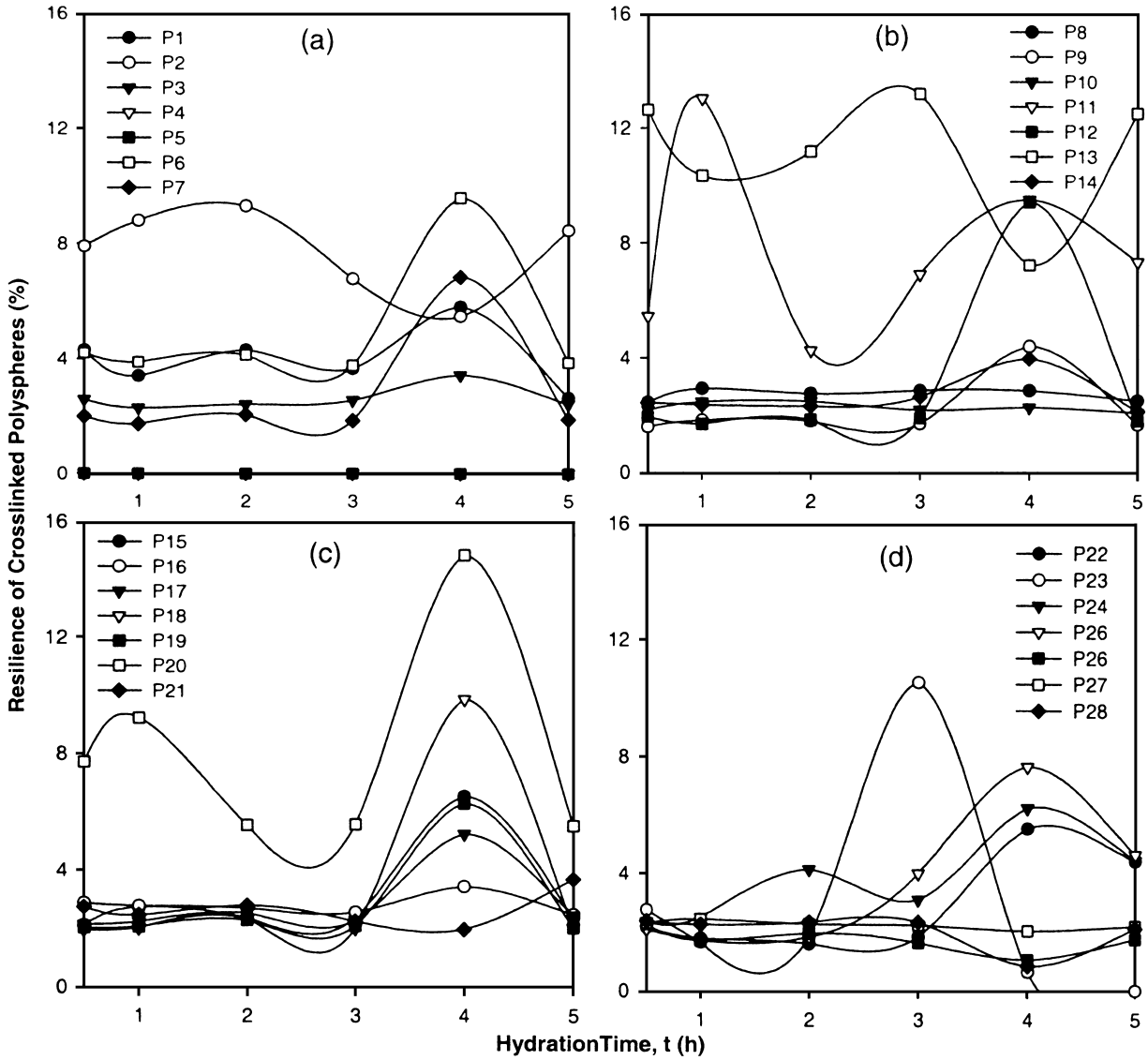

FIGURE 5 Matrix Resilience Profiles of the 28 Statistically Formulated Hydrated Polyspheres (N=10, S.D. <0.25 in All Cases).

particles having an average size of 1.5 mm (range from 0.95 mm to 2.05 mm). Surface examination revealed minor micro-indentations.

Macros created on Texture Exponent for Windows V3.2 (Stable Micro Systems, England) were run on the textural profiles to calculate various parameters, namely the hydrated matrix resilience, rupture energy, and primary fracture.

On hydration of the polyspheres, the matrix resilience (Fig. 5) significantly changed with time (e.g., P6, P11, P20), while in other cases the resilience remained constant (e.g., P10, P14, P27). In general, it was observed that in the absence of pectin, the resilience was highly variable, which may be attributed to the lower degree of crosslinking obtained with alginate. The contrary was observed when pectin was applied in the design. In these cases, the higher degree of crosslinking achieved resisted significant changes in matrix resilience.

In terms of the matrix rupture energy (i.e., the amountof energy required to rupture the unhydrated polyspheres), P7, P18, and P25 (Fig. 6) required the most work to be performed prior to their rupture. This may be attributed the strong crosslinks formed between the pectin monomers and Zn^{2+} ions; hence, stress on the crosslinked matrix was significantly shielded.

More energy was required to rupture the unhydrated polyspheres composed of pectin and the crosslinking agent (average of 0.097 J) than sodium alginate and

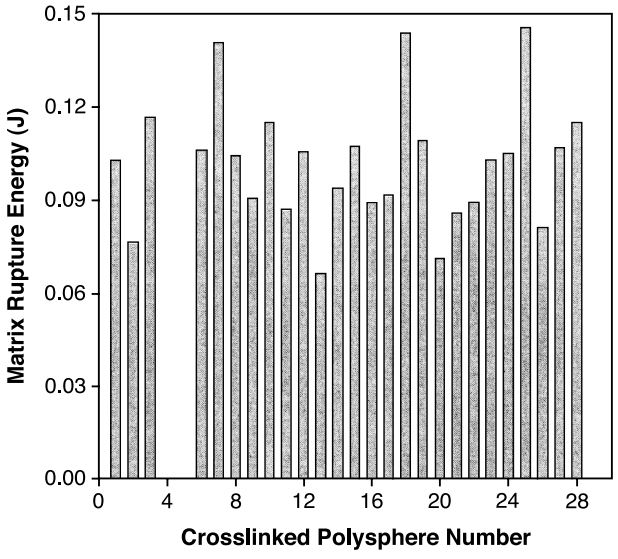

FIGURE 6 **Energy Associated with the Rupture of the Matrix on Application of a Destructive Force (P4 and P5 could not be Crosslinked, N=10, S.D. <0.007 in all cases).**

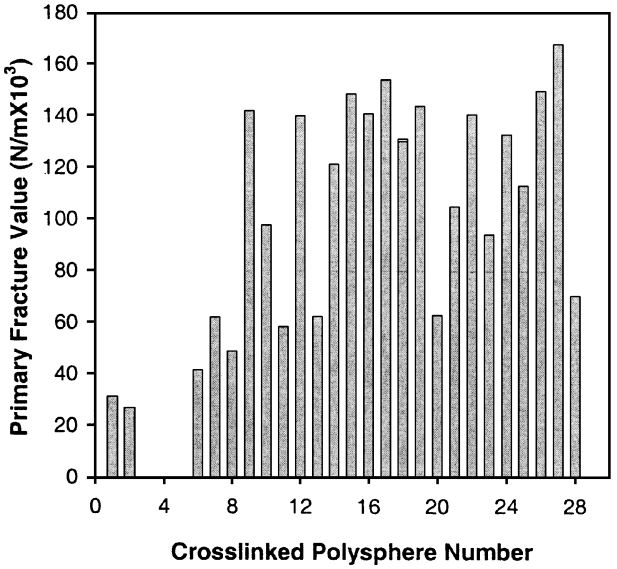

FIGURE 7 **Primary Facture of Matrix (P3 has a Very Low Fracture Value and Therefore cannot be Observed, P4 and P5 could not be Crosslinked, N=10, S.D. <0.9 in All Cases).**

the crosslinking agent. This however, was not significantly greater (p=0.098) than the energy (average of 0.082 J) required to rupture thealginate polyspheres. The slightly higher rupture energy could be attributed to the stronger crosslinks formed between the Zn^{2+} ions and pectin, than the Zn^{2+} ions and alginate. There was also no significant difference in the matrix rupture energy from the polyspheres crosslinked with Zn^{2+} ions either from the $ZnSO_4.7H_2O$ or $C_{12}H_{22}ZnO_{14}$ in both pectin (p=0.1248) or alginate (p=0.0713).

On the other hand, the primary fracture of the crosslinked matrix (Fig. 7) did not show any clear

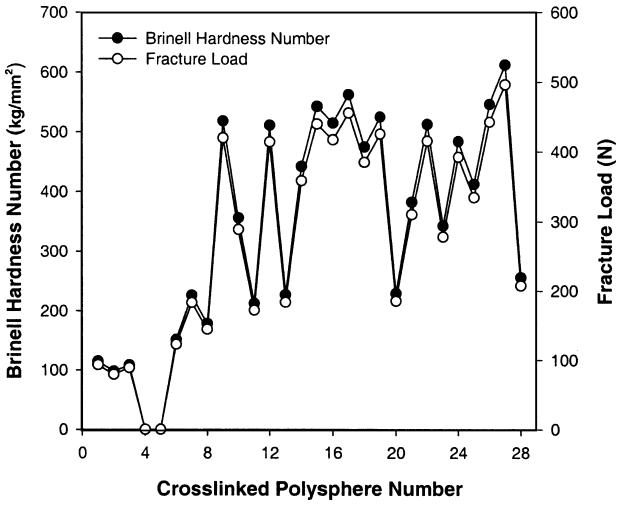

FIGURE 8 **Relationship Between Brinell Hardness and Fracture Load (N=10, S.D. <2).**

correlation with the resilience and rupture energy behavior. In this case it is believed that primary fracture is a surface phenomenon, rather than a result of a collapse of the internal crosslinked structure. The surfaces of the polyspheres were flawed with dispersions of the above-mentioned micro-indentations, which resembled minute peripheral defects with a concave shape. Such defects would ideally support the primary collapse phenomenon on application of low-level forces.

Statistical analysis of the primary fracture values for the 28 polyspheres tested revealed that in this case, however, there was a significant difference ($p=0.046$) between the primary fracture values of the crosslinked pectinate and alginate polyspheres. The average energy to produce a primary fracture was 102.85×103 N/m for the crosslinked pectinate polyspheres, and 50.26×103 N/m for the crosslinked alginate polyspheres. There was also a significant difference ($p=0.028$) in the primary fracture value of the pectinate polyspheres when they were crosslinked with Zn^{2+} either from $ZnSO_4.7H_2O$ or (average value of 69.11×103 N/m) or $C_{12}H_{22}ZnO_{14}$ (average value of 127.74×103 N/m). This may indicate that the large structure of the $C_{12}H_{22}ZnO_{14}$ molecule may attach itself to the peripheral zones of the polysphere.

Further studies revealed no overall statistical significance ($p=0.152$) between the Brinell hardness and fracture load profiles (Fig. 8) for each of the 28 crosslinked polyspheres. Using the number of degrees of freedom of 25 and probability level at $p=0.05$, the calculated correlation coefficient (R) by nonlinear regression was greater than the tabulated values provided in correlation tables ($R_{calculated}=0.997$, $R_{tabulated}=0.381$) Table of Correlation Coefficients. In this regard it became apparent that the correlation between the Brinell hardness and fracture load were significant. Essentially, these parameters further substantiate the highly variable stress-strain behavior of the polyspheres, a result directly related to the different crosslink densities depending on the crosslinker and polymer combinations employed.

Relationship Between Drug Encapsulation Efficiency and Matrix Rupture Energy

Polyspheres composed of higher levels of pectin (see Table 4) were able to encapsulate significantly lower quantities of drug, based on the presented crosslinking hypothesis and statistical analysis of drug encapsulation. This theory is further sustained by the fact that lower drug encapsulation at higher levels of pectin, and the subsequent inclusion of more Zn^{2+} ions, appeared to enhance the crosslink density of the matrix. Therefore, the trend observed in Fig. 8 reflects that polyspheres exhibiting lower drug entrapment, possessed greater rigidity, based on the large rupture energy values (Fig. 9). The Zn^{2+} ions preferentially occupy the spaces intended for the drug.

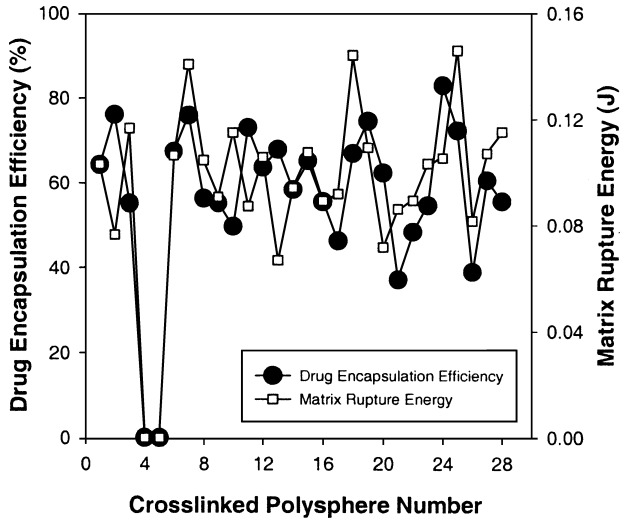

FIGURE 9 **Relationship Between the Potential of the Crosslinked Matrix to Rupture in the Presence of Internally Embedded Drug.**

Viscosity Changes of Sequentially Crosslinking Polymer Solutions

Four different and distinct viscosity patterns were observed during in situ crosslinking of polymer solutions (Fig. 10).

Figure 10a indicates an initial slow rate of change in the viscosity of the polymers involved. Upon reaching a threshold crosslinker value of approximately 2000 μL, the rate of polymeric entanglement rapidly progressed and peaked at 1300 cP. Subsequent addition of the crosslinker indicated a rapid decline in the viscosity, which is attributed to an aqueous dilution effect of the entire polymeric system (Pillay & Fassihi, 1999; Pillay et al., 2002). This was not a reflection of chain disentanglement.

Figure 10b indicates alarge lag-phase prior to any change in the viscosity. The threhold value in this case

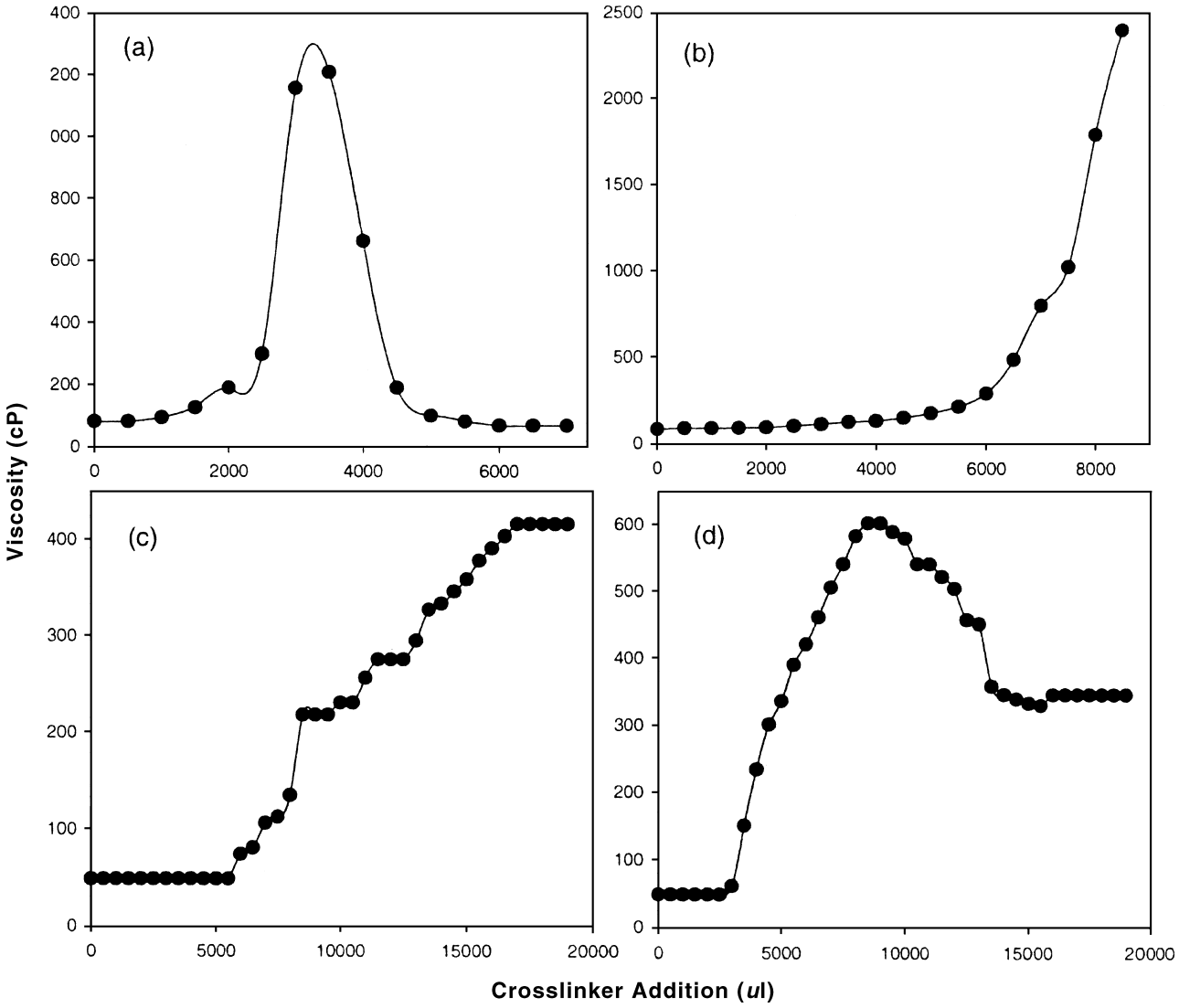

FIGURE 10 **Viscosity Transitions Displayed during Sequential Polymeric Chain Stiffening on Titration of the Crosslinking Agent(s). Typical Patterns Observed are: (a) Bell-Shaped, (b) Hyperbolic, (c) Sigmoidal, and (d) Incomplete Bell Curve (Abnormal Distribution).**

was approximately 6500 μL, indicating a significantly higher resistance to chain stiffening, contrary to that observed in Fig. 10a.

The threshold for chain stiffening shown in Fig. 10c is very similar to that observed in Fig. 10b (5500 μL). However, viscosity steadily increased over numerous titrations of the crosslinker and peaked at 416 cP. At the maximum, the viscosity remained constant despite additional crosslinker. This may be attributed to an influx of the crosslinking ions into the spongy, absorbent matrix and hence accounts for an absence of the aqueous dilution effect seen in Fig. 10a.

Figure 10d exhibits behavior very similar to that seen in Fig. 10a, except that after the aqueous dilution phase, beginning from 600 cP, the crosslinked matrix tends to become spongy at 350 cP and significantly absorbs the crosslinking ions. Hence, no change in viscosity was observed.

One of the limitations to single-point measurements is that this may not be an optimal choice for presumably non-Newtonian fluids.

Preoptimized Dissolution Responses Generated from the Box-Behnken Statistical Formulation Combinations

This investigation produced significantly different dissolution profiles for the 28 polysphere formulations

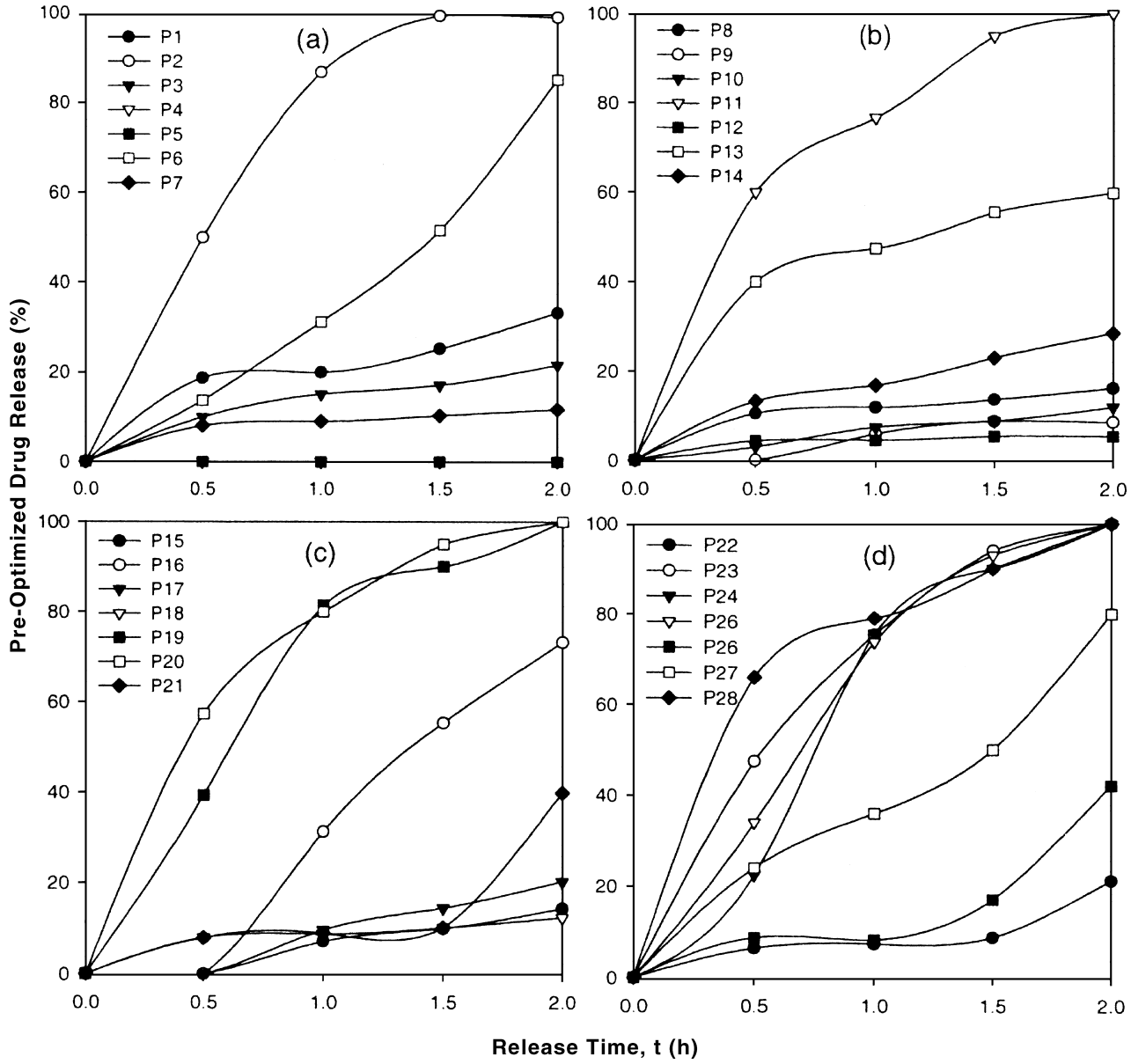

FIGURE 11 **Dissolution Profiles of the 28 Crosslinked Polysphere Formulations (a–d) in Phosphate Buffer pH 6.8 (N=3, S.D. <0.07 in All Cases).**

over a 2-h test period termed t_{2h} in this study, and was attributed to the different degrees of crosslinking achieved in each case (Fig. 11).

Our primary aim was to use the t_{2h} drug release values obtained, as a strategy to reduce the observed burst effects and subsequently optimize the profile by modulating its release over an extended period of time.

From a mechanistic viewpoint, the drug release function was primarily selected based on the fact that maximal polymeric hydration and swelling occurs within 2 h. These are dynamic processes that directly regulate drug release. The statistical considerations associated with our selection are discussed below.

Numerical Optimization of Drug Release

Tables 5 and 6 provide a detailed analysis of the mathematical fit of the in vitro dissolution response function Eq. 4 and the levels of significance for the various regression coefficients.

The least-squares fit showed a high correlation coefficient (R^2) of 0.93 (Table 5). In addition, the

TABLE 5 Diagnostics for a Complete Fit of the In Vitro Dissolution Response Function by Stepwise Forward and Backward Elimination Regression

Response	Response equation[a]	R^2	d[b]
In vitro dissolution	$b_0 + b_1 * ZnG * ZnG + b_2 * NaAl * P + b_3 * NaAl * ZnS + b_4 * NaAl * ZnG + b_5 * P * ZnS + b_6 * P * ZnG + b_7 * ZnS * ZnG$ (4)	0.93	0.95

[a]The abbreviated terms are described in the regression model Eq. 1.
[b]d is the Durbin-Watson Statistic.

Durbin-Watson Statistic, *d*, an index that quantifies the serial correlation of least-squares deviates, was close to 2, indicating that the estimates of the variances and covariances of the respoonse parameters have excellent correlation.

Table 6 indicates that only those terms containing the sodium alginate-$ZnSO_4.7H_2O$ (b_3), pectin-$ZnSO_4.7H_2O$ (b_5), pectin-$C_{12}H_{22}ZnO_{14}$ (b_6), and combination of the binary $ZnSO_4.7H_2O$-$C_{12}H_{22}ZnO_{14}$ crosslinker (b_7) were the most statistically significant ($p<0.05$). This also further reinforces the more prevalent interaction between Zn^{2+} and pectin, which results in optimal matrix crosslinking.

Based on the fact that the Box-Behnken design follows a quadratic model, we felt that it was most appropriate to employ the generalized reduced gradient (GRG2), nonlinear optimization algorithm to solve for drug release using constraints (independent variables) that regulat the three-dimensional configuration of the crosslinked matrix, and in effect drug dissolution.

The limitations (% w/v concentration) placed on the independent variables were based on recent work (Pillay & Danckwerts, 2002):

- $0 \leq [NaAl] \leq 2$
- $0 \leq [P] \leq 2$
- $0 \leq [ZnS] \leq 5$
- $0 \leq [ZnG] \leq 5$

The lower limits for both polymers and crosslinking agents (namely 0% w/v) were selected to test their absence in the crosslinking process. Polymer concentrations for sodium alginate and pectin beyond 2% w/v were not feasible, as accurate titration was significantly inhibited by their excessively high viscosity. The upper limits for the crosslinking agents were based on their ability to form stable solutions. Solutions above 5% w/v produced a yellow discoloration, indicating physicochemical instability.

Initially, test on the regression model Eq. 4 was conducted using theoretically fixed dissolution values (%) at t_{2h} selected over a range from low to high that would be representative of those typically observed either as a burst effect or suppressed release. The power of the model was evaluated by inputting these theoretical values into the GRG2 algorithm to generate the predicted dissolution values (Table 7).

The numerical solutions for the combination of the polymers and crosslinkers clearly indicated that the predicted values closely correlated with the fixed theoretical dissolution values at t_{2h} ($p>0.05$). Moreover, with higher input values for drug release at t_{2h}, the algorithm output indicated that lower concentrations of pectin were required in comparison to alginate. This further confirms the fact that in this binary matrix system, pectin is the key polymer responsible for controlling drug release. This infers that pectin, in comparison to alginate, is crosslinked to a larger extent by the Zn^{2+} ions.

The complete, experimentally derived dissolution profiles for the above-stated theoretical formulations (PA-PG), traced over a period of 7 days, are shown in

TABLE 6 Level of Significance of the Regression Coefficients Generated for the Quadratic Response Function at a 95% Confidence ($p<0.05$)

Coefficient	Independent variables	p-values
b_0	–	0.090
b_1	ZnG∗ZnG	0.229
b_2	NaAl∗P	0.365
b_3	NaAl∗ZnS	0.039
b_4	NaAl∗ZnG	0.993
b_5	P∗ZnS	0.003
b_6	P∗ZnG	0.006
b_7	ZnS∗ZnG	0.040

TABLE 7 Theoretical t_{2h} Values Numerically Predicted Using the GRG2 Algorithm

Theoretical polysphere	Fixed theoretical dissolution at t_{2h} (%) (input)	Predicted [Polymers] (% w/v)		Predicted [crosslinkers] (% w/v)		Predicted dissolution at t_{2h} (%) (output)
		[NaAl]	[P]	[ZnG]	[ZnS]	
PA	0	0	2	5	5	0
PB	2	0.35	2	2.50	3.12	2
PC	5	0.40	1.89	2.50	3.01	6
PD	10	0.50	1.65	2.49	2.80	15
PE	35	0.88	0.82	2.47	2.14	30
PF	75	1.34	0.02	2.51	1.85	77.99
PG	100	2	0	2.79	3.58	100

Fig. 12. Noteworthy is that tailor-made dissolution profiles can be achieved through robust statistical optimization, with zero-order drug release extending from several hours to days (simple Power Law n-exponent >0.95; linear regression $R^2>0.97$). The attainment of steady-release kinetics without a lag-phase over a period of several days marks significant progress made over previous studies outlined in the Introduction section. Furthermore, simulation studies predicted that polyspheres PA and PB may continue to release over several more days, $\approx$50 days for PA and $\approx$25 days for PB. In these cases, such prolonged zero-order release may be desirable in the design and development of implantable drug delivery devices.

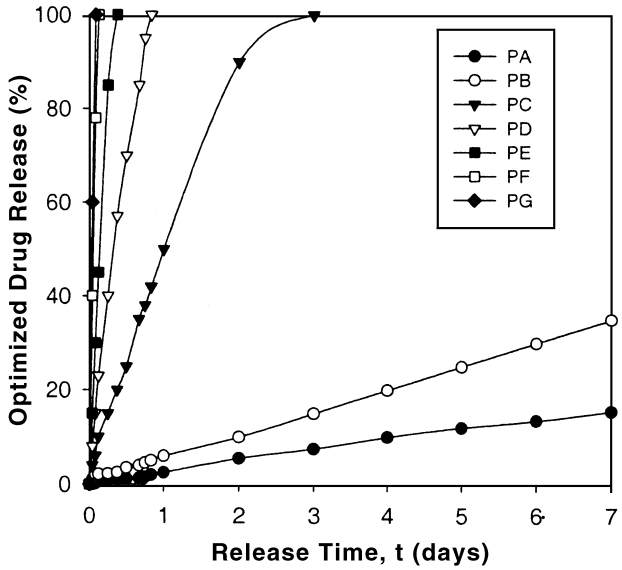

FIGURE 12 Experimentally Derived Dissolution Profiles in Phosphate Buffer pH 6.8 for Polyspheres PA-PG (N=3, S.D. <0.10 in All Cases).

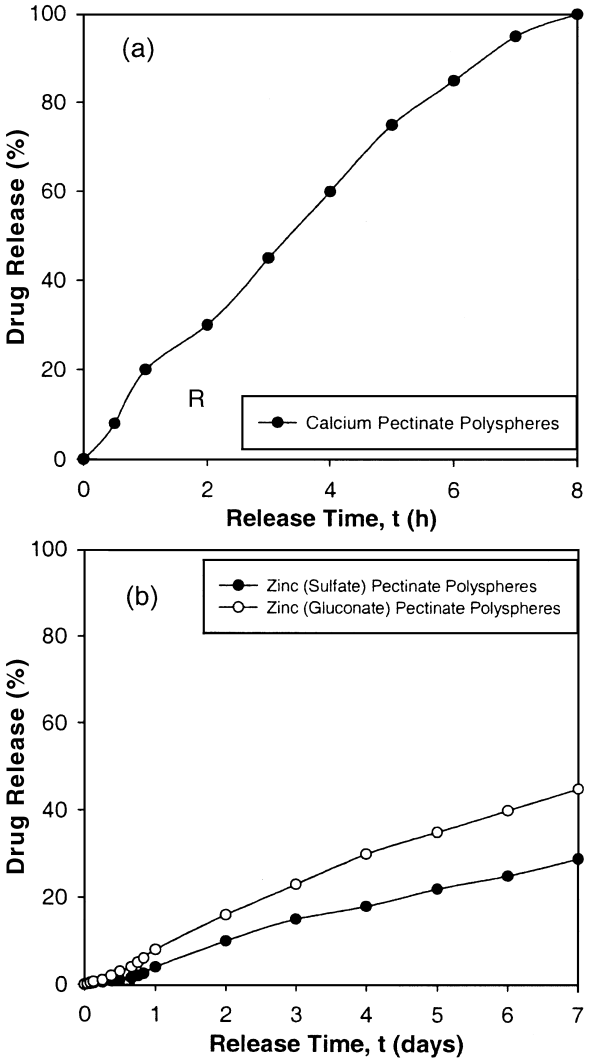

FIGURE 13 Drug Release Profiles from (a) Ca-Pectinate and (b) ZnS- and ZnG-Pectinate Polyspheres in Phosphate Buffer pH 6.8 (N=3, S.D. <0.35 in All Cases).

Proof of Concept: Superior Prolonged Zero-Order Drug Release from Crosslinked Alginate and Pectinate Matrices Using Zn^{2+} over Ca^{2+} Ions

In Section 4.1, based on the different coordination numbers and structural chemistry of Ca^{2+} and Zn^{2+} ions, it was hypothesized that the degree of crosslinking would be significantly greater with the use of Zn^{2+} ions in both alginate and pectin as opposed to using Ca^{2+}. Based on the dissolution experiments described previously (Fig. 13), it was observed that pectin, when crosslinked with Zn^{2+} ions, provided significantly greater reduction in drug release, as opposed to the use of alginate.

In order to test this hypothesis without optimization studies, but based purely on a formulation approach, polyspheres composed of 2% w/v of pectin were separately crosslinked with 5% w/v each of $CaCl_2$, $C_{12}H_{22}ZnO_{14}$, and $ZnSO_4.7H_2O$. It was observed that drug release from the pectinate matrices increased in the following order of the crosslinking ions employed: $CaCl_2$»$C_{12}H_{22}ZnO_{14}$>$ZnSO_4.7H_2O$ (Fig. 13a,b). Ca-pectinate matrices failed to sustain true prolonged drug release (100% released in 8 h).

CONCLUSIONS

In this study, the Box-Behnken experimental design has provided a rational approach to establish the effect of Zn^{2+} ions in achieving different degrees of crosslinking of alginate and pectin in the form of drug-encapsulated polyspheres. Using the experimental and predicted responses generated from a quadratic regression model in conjunction with statistical analyses revealed a more definitive answer as to why Zn^{2+} ions are superior to Ca^{2+}. The physicomechanical properties of crosslinked polyspheres have played a salient role in regulating their drug release potential, a relationship often overlooked. Hence, numerical optimization of dissolution data became more meaningful to employ in aiming for steady-state release. The outcome was proof of concept that linear drug release can be controlled over several days using crosslinked Zn-pectinate matrices, which prior to this work has not been demonstrated.

ACKNOWLEDGMENTS

This work was made possible through a grant from the National Research Foundation of South Africa (NRF 2053373). In addition, Dr. Zayniddin Muhidinov acknowledges the Fulbright Foundation (USA) for award of the Distinguished Visiting Professor fellowship.

REFERENCES

Aslani, P., & Kennedy, R. A. (1996a). Studies on diffusion in alginate beads. I. Effect of crosslinking with calcium or zinc ions on diffusion of acetaminophen. *Journal of Controlled Release, 42*, 75–82.

Aslani, P., & Kennedy, R. A. (1996b). Effect of gelation condition and dissolution media on the release of paracetamol from alginate gel beads. *Journal of Microencapsulation, 13*, 601–614.

Bock, C. W., Markham, G. D., Katz, A. K., & Glusker, J. P. (2003). The arrangement of first- and second-sphere water molecules in trivalent aluminum complexes: results from density functional theory and structural crystallography. *Inorganic Chemistry, 42*, 1538–1548.

Bonferoni, M. C., Rossi, S., Ferrari, F., Stavik, E., Pena-Romero, A., & Caramella, C. (2000). Factorial analysis of the influence of dissolution medium on drug release from carrageenan-diltiazem complexes. *AAPS PharmSciTech, 1*, 1–8.

Braccini, I., Grasso, R. P., & Perez, S. (1999). Conformational and configurational features of acidic polysaccharides and their interactions with calcium ions: a molecular modeling investigation. *Carbohydrate Research, 317*, 119–130.

Chan, L. W., Jin, Y., & Heng, P. W. S. (2002). Crosslinking mechanisms of calcium and zinc in production of alginate microspheres. *International Journal of Pharmaceutics, 242*, 255–258.

Chaplin, M. (2004). *Hofmeister Series*. http://www.lsbu.ac.uk/water/hofmeist.html. Accessed 28 October 2004.

Crichton, M., & Surita, B. (2003). Structure and intermicellar interactions in block polyelectrolyte assemblies. *Journal of Applied Crystallography, 36*, 652–655.

Crystal Structure of Calcium. http://www.webelements.com/webelements/elements/text/Ca/xtal.html 2004.

Crystal Structure of Zinc. http:/www.webelements.com/webelements/elements/text/Zn/xtal.html 2004.

Debon, S. J. J., & Tester, R. F. (2001). In vitro binding of calcium, iron and zinc by non-starch polysaccharides. *Food Chemistry, 73*, 401–410.

Dronnet, V. M., Renard, C. M. G. C., Axelos, M. A. V., & Thibault, J.-F. (1996). Characterisation and selectivity of divalent metal ion binding by citrus and sugar-beet pectins. *Carbohydrate Polymers, 30*, 253–263.

El-Gibaly, I. (2002). Oral delayed-release system based on Zn-pectinate gel (ZPG) microparticles as an alternative carrier to calcium pectinate for colonic drug delivery. *International Journal of Pharmaceutics, 232*, 199–211.

Franco, C. R., Chagas, A. P., & Jorge, R. A. (2002). Ion-exchange equilibria with aluminum pectinates. *Colloid Surfaces A: Physicochemical Engineering Aspects, 204*, 183–192.

Furlanetto, S., Maestrelli, F., Orlandini, S., Pinzauti, S., & Mura, P. (2003). Optimization of dissolution test precision for a ketoprofen extended-release product. *Journal of Pharmaceutical and Biomedical Analysis, 32*, 159–165.

George, P., Glusker, J. P., Markham, G. D., Trachtman, M., & Bock, C. W. (2003). An ab initio molecular orbital study comparing the

bonding of the NH_3 and the H_2O in the monoamines and the monohydrates of main group and transition metal ions. *Molecular Physics, 101*, 2451–2467.
Gray, C. J., & Dowsett, J. (1988). Retention of insulin in alginate gel beads. *Biotechnology and Bioengineering, 31*, 607–612.
Havel, J., & Hogfeldt, E. (1995). Evaluation of water sorption equilibrium data on Dowex ion exchanger using WSLET-MINUIT program. *Scripta of the Faculty of Science, Masaryk University, 25*, 73–84.
Ibanez, J. P., & Umetsu, Y. (2002). Potential of protonated alginate beads for heavy metals uptake. *Hydrometallurgy, 64*, 89–99.
Ionic Information of Calcium. http://ww.scescape.net/~woods/elements/calcium.html 2004.
Ionic Information of Zinc. http://www.scescape.net/~woods/elements/zinc.html 2004.
Jang, L. K., Nguyen, D., & Geesey, G. G. (1999). Selectivity of alginate gel for Cu over Zn when acidic conditions prevail. *Water Research, 33*, 2817–2825.
Kjoniksen, A.-L., Hiorth, M., Roots, J., & Nystrom, B. (2003). Shear-induced association and gelation of aqueous solutions of pectin. *Journal of Physical Chemistry B, 107*, 6324–6328.
Lavelle, L., & Fresco, J. R. (2003). Stabilization of nucleic acid triplexes by high concentration of sodium and ammonium salts follows the hofmeister series. *Biophysical Chemistry, 105*, 681–699.
Mayanovic, R. A., Anderson, A. J., Bassett, W. A., & Chou, I.-M. (2001). Hydrogen bond breaking in aqueous solutions near the critical point. *Chemistry and Physics Letters, 336*, 212–218.
McDowell, R. H. (1979). *Properties of Alginate* (4th ed.). London: Alginate Industries, p. 67.
Pillay, V., & Fassihi, R. (1999). In vitro release modulation from crosslinked pellets for site-specific drug delivery to the gastrointestinal tract. II. Physicochemical characterization of calcium-alginate, calcium-pectinate and calcium-alginate-pectinate pellets. *Journal of Controlled Release, 59*, 243–256.
Pillay, V., & Fassihi, R. (2001). Probing the dynamics of matrix hydration in the presence of electrolytes. *Drug Delivery, 4*, 87–92.
Pillay, V., & Danckwerts, M. P. (2002). Textural profilingand statistical optimization of crosslinked calcium-alginate-pectinate-cellulose acetophthalate gelisphere matrices. *Journal of Pharmaceutical Sciences, 91*, 2559–2570.
Pillay, V., Danckwerts, M. P., & Fassihi, R. (2002). A crosslinked calcium-alginate-pectinate-cellulose acetophthalate gelisphere system for linear drug release. *Drug Delivery, 9*, 77–86.
Plumridge, T. H., Steele, G., & Waigh, R. D. (2000). Geometry-based simulation of the hydration of small molecules. *Physical Chemistry Communications, 8*, 1–6.
Prakobvaitayakit, M., & Nimmannit, U. (2004). Optimization of polylactic-co-clycolic acid nanoparticles containing itraconazole using 2^3 factorial design. *AAPS PharmSciTech, 4*, 1–9.
Table of Correlation Coefficients. http:/helios.bto.ed.ac.uk/bto/statistics/tress11.html.
Terentjev, E. M., Hotta, A., Clarke, S. M., & Warner, M. (2003). Liquid crystalline elastomers: dynamics and relaxation of microstructure. *Philosophical Transactions of the Royal Society of London, 361*, 1–12.
Tiitu, M., Hiekkataipale, P., Hartikainen, J., Malkela, T., & Ikkala, O. (2002). Viscoelastic and electrical transitions in gelation of electrically conducting polyaniline. *Macromolecules, 35*, 5212–5217.
Wang, X.-B., Yang, X., Nicholas, J. B., & Wang, L.-S. (2001). Bulk-like features in the photoemission spectra of hydrated doubly charged anion clusters. *Science, 294*, 1322–1325.
Wilding, I. R., Coupe, A. J., & Davis, S. S. (2001). The role of gamma-scintigraphy in oral drug delivery. *Advanced Drug Delivery Reviews, 46*, 103–124.